Hindawi Publishing Corporation
International Journal of Quality, Statistics, and Reliability
Volume 2010, Article ID 180293, 9 pages
doi:10.1155/2010/180293

Research Article

Effectively Monitoring the Performance of Integrated Process Control Systems under Nonstationary Disturbances

Karin Kandananond

Faculty of Industrial Technology, Valaya Alongkorn Rajabhat University (VRU). 1 Moo 20 Phaholyothin Road, Klongluang, Pathum Thani 13180, Thailand

Correspondence should be addressed to Karin Kandananond, kandananond@hotmail.com

Received 13 December 2009; Accepted 8 July 2010

Academic Editor: Shuen-lin Jeng

The objective of this paper is to quantify the effect of autocorrelation coefficients, shift magnitude, types of control charts, types of controllers, and types of monitored signals on a control system. Statistical process control (*SPC*) and automatic process control (*APC*) were studied under non-stationary stochastic disturbances characterized by the integrated moving average model, *ARIMA* $(0, 1, 1)$. A process model was simulated to achieve two responses, mean squared error (*MSE*) and average run length (*ARL*). A factorial design experiment was conducted to analyze the simulated results. The results revealed that not only shift magnitude and the level of autocorrelation coefficients, but also the interaction between these two factors, affected the integrated system performance. It was also found that the most appropriate combination of *SPC* and *APC* is the utilization of the minimum mean squared error (*MMSE*) controller with the Shewhart moving range (*MR*) chart, while monitoring the control signal (X) from the controller. Therefore, integrating *SPC* and *APC* can improve process manufacturing, but the performance of the integrated system is significantly affected by process autocorrelation. Therefore, if the performance of the integrated system under non-stationary disturbances is correctly characterized, practitioners will have guidelines for achieving the highest possible performance potential when integrating *SPC* and *APC*.

1. Introduction

Better quality leads to cost reduction. The two major techniques used to monitor and reduce the variation in manufacturing processes are statistical process control (*SPC*) and automatic process control (*APC*). The *SPC* method separates assignable causes from common causes. Shewhart control charts are traditional *SPC* tools based on the assumption that each observation is uncorrelated. However, the independence assumption is violated in many scenarios, especially in continuous process industries where advanced measurement technologies and shortened sampling intervals are used. Under normal, uncorrelated conditions, the process model has a fixed mean (μ), and the fluctuation around the mean is the result of white noise (a_t). A process model of *SPC* can be expressed as follows:

$$Y_t = \mu + a_t. \tag{1}$$

However, when observations are correlated, the correlation structure and drift in the mean are characterized by disturbances. If process observations vary around a fixed mean and have a constant variance, this type of variability is called the stationary behaviour. Otherwise, the behaviour is non-stationary. MacGregor [1] indicated that there are two types of disturbances, deterministic and stochastic disturbances. Stochastic disturbances are random and might be stationary or non-stationary, while deterministic disturbances are a step shift or ramp in the process mean. Box and Jenkins

[2] introduced a stochastic difference equation that can model stochastic disturbances. This equation has been used to forecast one-step ahead disturbances, according to the data characteristics of stationary or non-stationary. The stochastic difference equation is expressed in the form of an autoregressive integrated moving average model, *ARIMA (p, d, q)*, as follows:

$$\Delta_d Y_t = \mu + \phi_1 \Delta_d Y_{t-1} + \phi_2 \Delta_d Y_{t-2} + \cdots + \phi_p \Delta_d Y_{t-p} + a_t - \theta_1 a_{t-1} - \cdots - \theta_q a_{t-q}. \quad (2)$$

The *ARIMA (p, d, q)* model indicates p as the order of the autoregressive part, d as the amount of difference, and q as the order of the moving average part. Mostly, non-stationary disturbances are modelled using the integrated moving average equations, *ARIMA (0, 1, 1)* or *IMA (1, 1)*, as recommended by Montgomery et al. [3] and Box and Luceno [4]. *IMA (1, 1)* is a special form of the *ARIMA (1, 1, 1)* model, with $\phi = 0$. The *ARIMA* model is considered a powerful method to solve the correlation problem, especially when it is applied to improve the capability of control charts to monitor the autocorrelated processes.

Application of an *ARIMA* model to *SPC* was reported by Lu and Reynolds [5]. Autocorrelated observations were characterized by an *ARIMA* model and an exponentially weighted moving average (*EWMA*) chart was utilized to monitor the residuals, based on the *ARIMA* model forecast values. Similarly, English et al. [6] compared the performance of the $\overline{X}$ and the *EWMA* chart under an autocorrelated process. Moreover, whether the *SPC* control chart should be used to monitor the error signal (e_t) or the control signal (X_t) is debatable, as highlighted by Montgomery [7].

An alternative to *SPC*, automatic process control (*APC*), was developed to monitor and control processes irrespective of the pattern of observed data. For *APC*, frequent process adjustments keep the output on the desired target. Taguchi et al. [8] suggested that the uniform quality of products is achieved by making adjustments according to process information. One example is the error of a watch, which is a function of time. Since both good and poor quality watches can be calibrated as needed, there is no difference between the quality of these two watches. Therefore, quality is not only a function of design, but also a function of the control system. According to Box and Luceno [4], two types of controllers, minimum mean squared error (*MMSE*) and proportional integral (*PI*), have been widely used in manufacturing processes to reduce variation due to autocorrelated disturbances. The control action from these controllers is known to whiten disturbances and only leaves random residuals. A *PI* controller is more robust than an *MMSE* controller, since it can compensate for unexpected mean shifts. However, Jiang and Tsui [9] claimed that the robustness of a *PI* controller makes it difficult to detect a mean shift in an autocorrelated process. For this reason, the selection of an appropriate controller is still an open issue for discussion.

While *APC* effectively reduces predictable quality variations, *SPC* monitors the process to detect unexpected causes of variation. *APC* responds to regulate the output response when there is a deviation from the target. Therefore, integrating *SPC* and *APC* could lead to a substantial improvement in process quality, since they complement each other. Numerous efforts have been attempted to assess the performance of an integrated system. Montgomery et al. [3] used a Shewhart chart, with *EWMA* and cumulative sum (*CUSUM*) charts to monitor the output deviation from the target when there are different sizes of process mean shifts. The *MMSE* controller was used to compensate for disturbances. The performance measurement was the average run length (*ARL*) and the average squared deviation from the target measured performance. Nembhard [10] utilized state-space equations to model dynamic processes while disturbances were characterized by *ARIMA* model. The integrated system was the combination of *PI* controller with Shewhart and *EWMA* charts. For a case study, Capilla et al. [11] deployed an *MMSE* controller with *CUSUM* and *EWMA* charts to monitor polymer viscosity in a reactor in which *AR* (1) and *ARMA (1, 1)* models were utilized to represent disturbances. The results showed that the integrated system can effectively minimize the variability of viscosity, while process shift can be detected rapidly.

According to Gultekin et al. [12], the combination use of *PI* controller and control charts (Shewhart and *CUSUM*) was initiated to reduce the output variation of continuously stirred tank reactors caused by deterministic disturbances and random input disturbances. By using a simulation, the integration was proved that it can reduce the mean squared error by 81% compared to the utilization of *PI* controller alone. Runger et al. [13] compared the performance of *MMSE* and *PI* controller when *EWMA* chart was utilized. The mathematical models of each control policy were derived and the comparison was done analytically. The disturbances were represented by *IMA (1, 1)* model and different shift magnitudes. Kandananond [14] performed the economic analysis to determine the optimal combination of controller and *SPC* chart which minimized the mean squared error of the output and average run length. For different models of disturbances, Kandananond [15] conducted the experimental analysis to assess the performance of the integrated system when disturbances followed *ARMA (1, 1)* model. For related publications, see Jiang and Tsui [9], MacGregor [16], Harris and Ross [17], Janakiram and Keats [18], Duffuaa et al. [19], Bisgaard and Kulachi [20], and Triantafyllopoulos et al. [21].

According to the above discussion, a limited amount of research has been conducted to characterize the statistical performance of integrated systems. The purpose of this paper is to study the effects of assignable causes (shift), levels of disturbance coefficients, types of controllers, types of control charts, and types of monitored signals on autocorrelated processes by using factorial experimental design. With this research, practitioners will have guidelines to achieve the highest performance of integrating *SPC* and *APC*.

2. Process Background

The basis of the analysis in this paper is a mathematical model used to study process autocorrelation effects on the

integrated process control system performance. The autocorrelation level of process outputs was controlled by adjusting the *IMA* coefficient. The autocorrelation behaviour is known to significantly downgrade the performance of control charts since the control limits of control charts are narrower than expected and might signal false alarms more frequently. Moreover, the situation could be more complicated when a shift occurs in the autocorrelated process. Two types of responses, mean squared error (*MSE*) and average run length (*ARL*), are obtained in order to assess the sensitivity and adjust the ability of the integrated system when there is a shift in the autocorrelated process.

2.1. Process Description. The autocorrelated process used was a continuous process with only one quality characteristic, represented by Y. Adjustments were made automatically by two types of controllers, minimum mean squared error (*MMSE*) and proportional integral (*PI*), in order to keep the process mean as close as possible to the target (T). As a shift occurred in the process, the moving range (*MR*) chart and exponentially weighted moving average (*EWMA*) were utilized to monitor the individual measurement of process mean to detect a shift.

2.2. Process Model. The observation of a process is considered from period 1 to 100 ($t = 1, 2, 3, \ldots, 100$) and the process description for observation *t+1* (Y_{t+1}) equals

$$Y_{t+1} = T + N_{t+1} + \delta(t) + gX_t. \tag{3}$$

The source of autocorrelation is process disturbances, characterized by the integrated moving average model, *ARIMA (0, 1, 1),* as follows:

$$N_{t+1} = N_t + a_{t+1} - \theta a_t, \quad -1 < \theta < 1, \tag{4}$$

where N_{t+1}, N_t are disturbances at time $t+1$ and t respectively, a_{t+1}, a_t are random errors at time $t+1$ and t, respectively, and θ is the moving average (*MA*) parameter which ranged from -1 to 1.

After an assignable cause occurs in the process, a shift of size δ_0 in the form of a step function is injected into a process as follows:

$$\delta(t) = \begin{cases} 0, & t < t_0, \\ \delta_0, & t \geq t_0, \end{cases} \tag{5}$$

where δ_0 is the magnitude of a shift, t_0 is the time that a shift occurs.

When the process mean is off target, each type of controller is utilized to compensate for disturbances and shifts. The derivation of the *MMSE* controller proceeds as follows.

Rearrange (3) as follows:

$$Y_{t+1} - T = N_{t+1} + \delta(t) + gX_t. \tag{6}$$

The deviation from the target ($Y_{t+1} - T$) should be minimized, so the possible value of X_t follows (7) as follows:

$$N_{t+1} + \delta(t) + gX_t = 0. \tag{7}$$

However, the future value of $\delta(t)$ and the value of disturbance in the next time frame are unknown, so these values are set to their minimum *MSE* forecasts. As a result, the value of X_t should be chosen such that

$$\hat{N}_{t+1|t} + gX_t = 0, \tag{8}$$

where $\hat{N}_{t+1|t}$ is the *MMSE* forecast of the disturbance. According to Box and Jenkins [2], the predicted disturbance equals

$$\hat{N}_{t+1|t} = (1 - \theta)N_t + \theta\hat{N}_{t|t-1}. \tag{9}$$

Substituting the disturbance N_t,

$$\hat{N}_{t+1|t} = (1 - \theta)(Y_t - T - \delta(t) - gX_{t-1}) + \theta\hat{N}_{t|t-1}. \tag{10}$$

Since the value of $\delta(t)$ is unknown, it is set to zero. For the *MMSE* controller, the adjustment signal (X_t) for disturbances following the *ARIMA (0, 1, 1)* model is expressed as follows:

$$X_t = X_{t-1} - \frac{1 - \theta}{g}(Y_t - T). \tag{11}$$

For *PI* controller, the optimal control signal is

$$X_t = X_{t-1} - G(Y_t - T + P\nabla Y_{t-1}). \tag{12}$$

Since the target (T) in this study is equal to zero, equation (12) is simplified to

$$X_t = X_{t-1} - G(Y_t + P\nabla Y_{t-1}). \tag{13}$$

The values of G and P are numerically calculated to minimize the output response and control signal variances by following this constraint

$$\min_{G,P}\left\{\frac{\mathrm{Var}(Y_t)}{\sigma_a^2} + \alpha\frac{\mathrm{var}(\nabla X_t)}{\sigma_a^2}\right\}, \tag{14}$$

where σ_a^2 is the variance of output error, Y_t is the process output.

After the adjustment has been performed, the error signal (e_t) is given by

$$e_t = Y_t - T. \tag{15}$$

Both control signal (X_t) and error signal (e_t) are monitored by a Shewhart moving range (*MR*) chart and an exponentially weighted moving average (*EWMA*) chart. The control limits for a moving range chart are

$$\begin{aligned} \text{Upper Control Limit (UCL)} &= \overline{Y} + 3\frac{\overline{MR}}{d_2}, \\ \text{Center line (CL)} &= \overline{Y}, \\ \text{Lower Control Limit (LCL)} &= \overline{Y} - 3\frac{\overline{MR}}{d_2}, \end{aligned} \tag{16}$$

where $\overline{Y}$ is the process mean and equals $\sum_{t=1}^{n} Y_t/n$, $MR = |Y_t - Y_{t-1}|$, $\overline{MR}$ is the average of moving average, $d_2 = 1.128$.

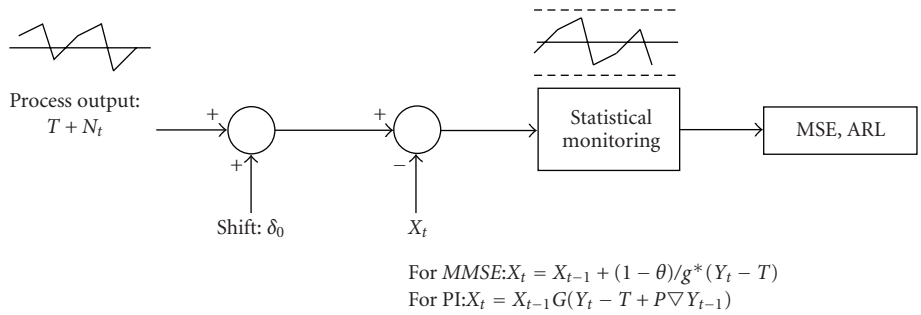

Figure 1: Schematic presentation of the process model.

For an *EWMA* chart, the control limits are expressed as follows:

$$\text{Upper Control Limit (UCL)} = \mu_0 + L\sigma\sqrt{\frac{\lambda}{(2-\lambda)}\left[1-(1-\lambda)^{2i}\right]},$$

$$\text{Center line (CL)} = \mu_0,$$

$$\text{Lower Control Limit (LCL)} = \mu_0 - L\sigma\sqrt{\frac{\lambda}{(2-\lambda)}\left[1-(1-\lambda)^{2i}\right]}, \tag{17}$$

where μ_0 is the average of preliminary data, L is the width of control limits, and λ is the weight assigned to the observation. The values of L and λ used were recommended by Lucas and Saccucci [22].

The mean squared error (*MSE*) is a method for evaluating a controller and is expressed as follows:

$$MSE = \frac{1}{n}\sum_{t=0}^{n}(Y_t - T)^2, \tag{18}$$

at the end of observation period ($n = 100$). On the other hand, the performance of a control chart is measured by the average run length (*ARL*), which is the expected number of samples taken before a shift is detected. Figure 1 shows the schematic presentation of the process model.

3. Simulation Modelling and Experiment

A factor screening experiment was designed using a statistical package, Design Expert Version 7.1, to analyze the effect of the autocorrelation and other factors on the responses. The selected design was a 2^5 full factorial design with a total of 32 runs. The selected factors were the *MA* parameters (θ), shift sizes, types of controllers, types of control charts, and types of signals. The two responses were mean squared error (*MSE*) and average run length (*ARL*). Each factor was set to high and low levels as shown in Table 1. θ was set to -0.9 and 0.9 for low and high values, respectively, since θ in the *ARIMA (0, 1, 1)* model is restricted to the range $-1 < \theta < 1$. Additionally, shift sizes of 0.5 σ_a and 3.5 σ_a were utilized to represent small and large shifts. Two types of control charts, a Shewhart moving range (*MR*) chart and an exponentially weighted moving average (*EWMA*) chart, were deployed in order to monitor control signal (X_t) and error signal (e_t) after the adjustment by the *MMSE* and *PI* controllers.

Table 1: Input factors and levels used in this experiment.

Factor	Low	High
A (*MA* parameter; θ)	-0.9	0.9
B (Shift magnitude)	0.5 σ_a	3.5 σ_a
C (Types of controllers)	*MMSE*	*PI*
D (Types of charts)	*MR*	*EWMA*
E (Output signals)	Control (X)	Error (e)

Regarding the simulation, each run was composed of 10,000 iterations which have been accomplished by using Palisade's @Risk Version 5.0. The random errors (a_t) from each period were simulated by following normal distribution with zero mean and a constant variance as follows:

$$a_t \sim N(0, \sigma_a^2). \tag{19}$$

The simulation results and the analysis of each response are shown in the following section.

4. Performance Analysis

The performance analysis was conducted to examine the effect of input factors on the responses. The statistical design is 2^5 factorial and the design matrix for all factors and the corresponding responses are shown in Table 2. For each response, the analysis of variance (*ANOVA*) approach was utilized to reveal the significant factors and their interactions. Model adequacy checking was performed to ensure that *ANOVA* assumptions were not violated and that there were no residual outliers.

4.1. Analysis of Mean Squared Errors (MSE). According to the half normal plot in Figure 2, the types of controllers (C) contribute the highest effect on the average *MSE*, followed by shift sizes (B), θ (A) and types of signals (E) in that order. Moreover, on the basis of the analysis of variance (*ANOVA*) in Table 3, the interaction effects exist and are based mostly on the above factors, with the highest-order term being *BCDE*. As a result, types of charts (D) and the interactions *BD*, *BE*, *CD*, *CE*, *BCD*, *BCE*, *BDE*, and *CDE* are included in the model even though they do not have small p-values. The

Table 2: Design matrix for *MSE* and *ARL* responses.

Run	θ	Shift	Controller	Chart	Signal	*MSE*	*ARL*
1	−0.9	0.5	*MMSE*	*MR*	*X*	1.0399	3.3118
2	0.9	0.5	*MMSE*	*MR*	*X*	1.0059	2.9221
3	−0.9	3.5	*MMSE*	*MR*	*X*	2.4003	1.6406
4	0.9	3.5	*MMSE*	*MR*	*X*	1.1816	1.4639
5	−0.9	0.5	*PI*	*MR*	*X*	2.2775	2.3706
6	0.9	0.5	*PI*	*MR*	*X*	2.4249	40.091
7	−0.9	3.5	*PI*	*MR*	*X*	2.5114	1.8625
8	0.9	3.5	*PI*	*MR*	*X*	2.7411	3.1661
9	−0.9	0.5	*MMSE*	*EWMA*	*X*	1.0496	1.022
10	0.9	0.5	*MMSE*	*EWMA*	*X*	1.0057	3.9966
11	−0.9	3.5	*MMSE*	*EWMA*	*X*	3.3105	1.088
12	0.9	3.5	*MMSE*	*EWMA*	*X*	1.6354	7.088
13	−0.9	0.5	*PI*	*EWMA*	*X*	2.2815	1.13847
14	0.9	0.5	*PI*	*EWMA*	*X*	2.9488	12.9762
15	−0.9	3.5	*PI*	*EWMA*	*X*	2.5028	1.288
16	0.9	3.5	*PI*	*EWMA*	*X*	2.7265	2.3726
17	−0.9	0.5	*MMSE*	*MR*	*e*	1.016	44.582
18	0.9	0.5	*MMSE*	*MR*	*e*	1.0142	44.4238
19	−0.9	3.5	*MMSE*	*MR*	*e*	2.9132	3.9047
20	0.9	3.5	*MMSE*	*MR*	*e*	1.2108	4.1644
21	−0.9	0.5	*PI*	*MR*	*e*	2.2805	24.3335
22	0.9	0.5	*PI*	*MR*	*e*	2.4241	49.8283
23	−0.9	3.5	*PI*	*MR*	*e*	2.4768	12.2195
24	0.9	3.5	*PI*	*MR*	*e*	2.5893	44.8057
25	−0.9	0.5	*MMSE*	*EWMA*	*e*	1.0147	47.6678
26	0.9	0.5	*MMSE*	*EWMA*	*e*	1.0142	44.8582
27	−0.9	3.5	*MMSE*	*EWMA*	*e*	2.4802	24.6955
28	0.9	3.5	*MMSE*	*EWMA*	*e*	1.214	1.7545
29	−0.9	0.5	*PI*	*EWMA*	*e*	2.2857	22.2706
30	0.9	0.5	*PI*	*EWMA*	*e*	2.4279	51
31	−0.9	3.5	*PI*	*EWMA*	*e*	2.5011	9.4092
32	0.9	3.5	*PI*	*EWMA*	*e*	2.6726	29.4745

hierarchical principle indicates that if there is a high-order term in the model, it will contain all the lower-order terms which compose it.

As shown in Figure 3, at the high level shift size (3.5), the average *MSE* is maximized when θ is highly negative ($\theta = -0.9$) while the minimum average *MSE* is achieved at $\theta = 0.9$. However, there is no significant difference in the average *MSE* at the low level shift size (0.5). The contour plot in Figure 4 also points out that there is a strong interaction between shift sizes and the level of autocorrelation (θ). The average *MSE* is maximized only when shift size is large (3.5) and θ is low (-0.9). At the high θ level (0.9), it is interesting to note that the average *MSE* is minimized even when the shift size is large (3.5).

Due to the cube plot in Figure 5, the average *MSE* when the *MMSE* controller is utilized is significantly lower than the ones when the *PI* controller is a part of the integrated system at both the low and high shift levels (0.5 and 3.5). Therefore, the *MMSE* controller should be the most appropriate controller to keep the process mean on the target. This result has been confirmed by the interaction plot between types of controllers and types of charts in Figure 6. The best result (minimum average *MSE*) is achieved when *MMSE* controller is selected.

According to the cube plots (Figure 7), the interaction between shift magnitude (B), controllers (C), and control charts (D) is shown at different levels of θ, when the effect from types of signals (E) is averaged. At the low level of θ (-0.9), the minimum average *MSE* (1.02902) is obtained at the low level of shift magnitude when *MR* chart is integrated with *MMSE* controller. At the high level shift size (3.5), *MR* chart with *MMSE* controller is still an appropriate choice to minimize average *MSE*, since the average *MSE* (2.47177) is lower than those occurring when a *PI* controller or an *EWMA* chart is utilized (2.48747, 2.50857, and 2.93032, resp.). At the high θ level (0.9), when an integrated system is

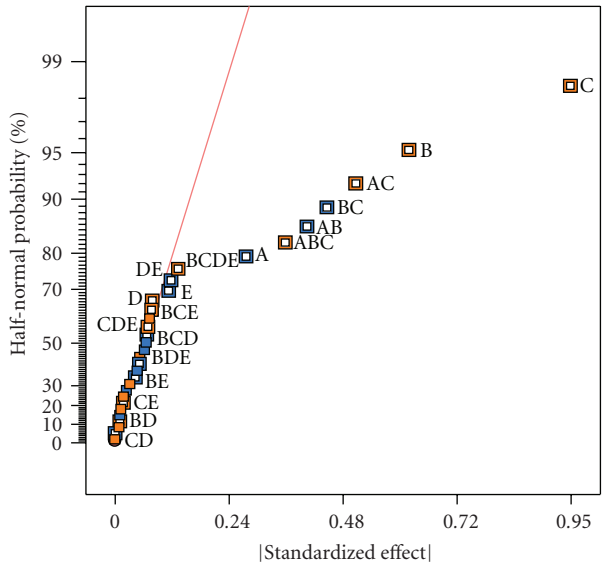

Figure 2: Half-normal plot of effects (for *MSE* response).

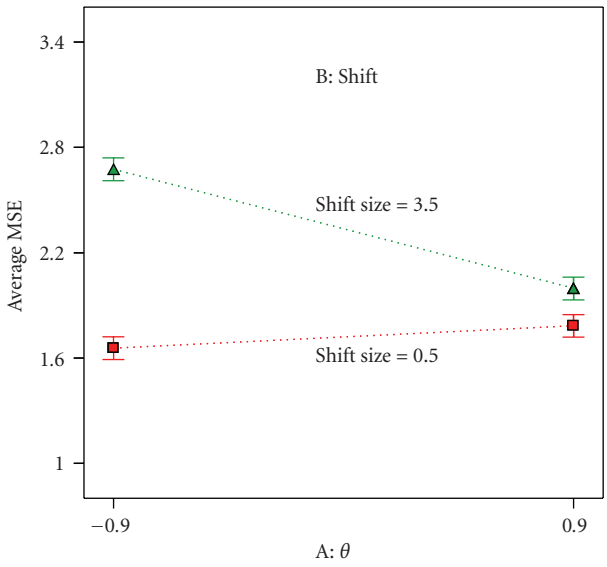

Figure 3: Interaction plot of θ and shift sizes (for *MSE* response).

composed of an *MMSE* controller and *MR* chart, the average *MSE* is still minimized and disregards shift magnitude.

4.2. Analysis of Average Run Length (ARL). The half-normal plot (Figure 8) indicates that θ (A), shift sizes (B), types of signals (E) contribute the significant main effects, and there are interactions involving some of these factors with the highest order term being *BCE*. Results from the analysis of variance (*ANOVA*) in Table 4 also confirm that these three factors and the interaction *BCE* are statistically significant, since their P-values are small. Similar to the analysis of *MSE*, the main effect from controller (C) and interactions *BC* and *CE* are included in the model because of the hierarchical principle.

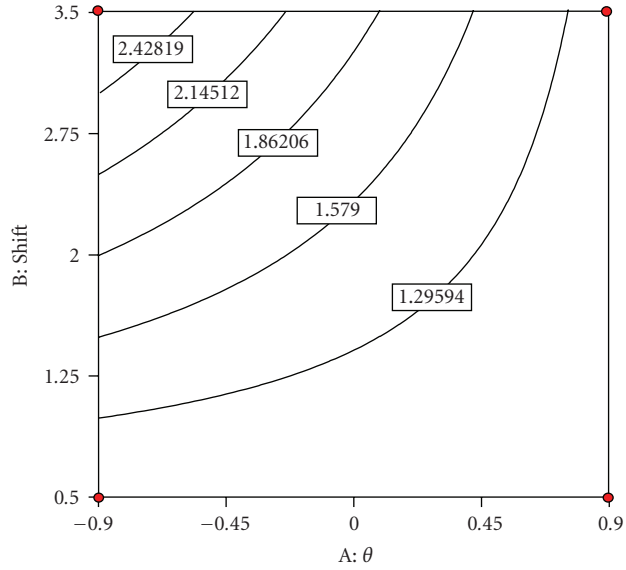

Figure 4: Contour plot of θ and shift sizes (for *MSE* response).

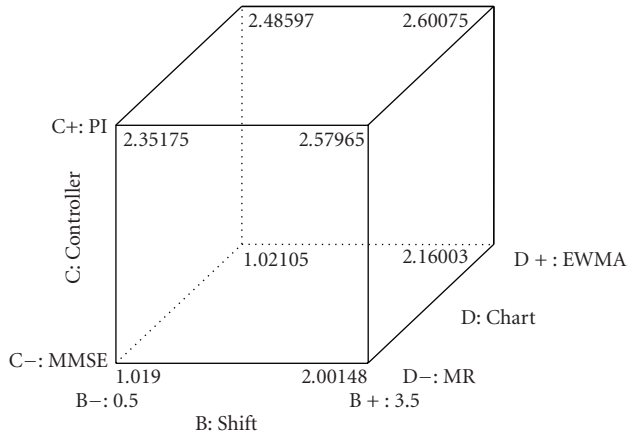

Figure 5: Cube plot of the *BCD* interaction (for *MSE* response).

As shown in Figure 9, the cube plot shows the *ARLs* at different levels of shift sizes (B), types of controllers, (C) and types of signals (E).

According to the plot, the *ARLs* (14.1441, 2.1723, 2.81313, 2.82013) when control signal (X) is monitored are shown to be significantly lower than those (36.8581, 23.9772, 8.62977, 45.383) when the error signal (e) is observed. These results signify that it is correct to assign the control signal to be monitored by the integrated system.

Another point of interest is that *ARL* is shown to be sensitive to types of controllers. At the low level shift (0.5), when *MMSE* controller is utilized and control signal is monitored, the *ARL* is only 2.81313. However, the effect tends to increase to 14.1441 when all situations are the same, but the *PI* controller is integrated with *SPC*. However, there is no significant difference at the high level of shift (2.82013 and 2.1723). This indicates that the *MMSE* controller should be selected as a part of the integrated system because it can keep *ARL* at a low level.

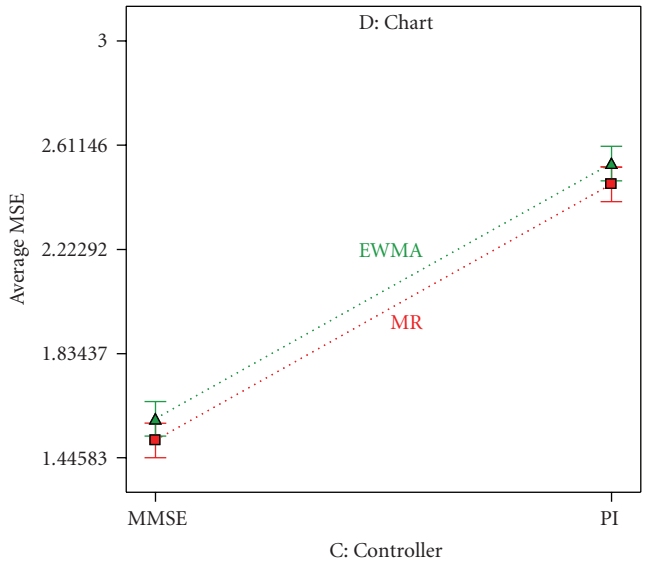

Figure 6: Interaction plot of controllers and control charts (for *MSE* response).

Table 3: *ANOVA* for *MSE*.

Source	Sum of Squares	Df	Mean Square	*F* Value	*P*-value
A-θ	0.6063	1	0.6063	43.3662	< .0001
B-Shift	3.0360	1	3.0360	217.1522	< .0001
C-Controller	7.2831	1	7.2831	520.9385	< .0001
D-Chart	0.0499	1	0.0499	3.5695	.0832
E-Signal	0.1022	1	0.1022	7.3074	.0192
AB	1.2982	1	1.2982	92.8550	< .0001
AC	2.0405	1	2.0405	145.9471	< .0001
BC	1.5820	1	1.5820	113.1569	< .0001
BD	0.0009	1	0.0009	0.0673	.7997
BE	0.0151	1	0.0151	1.0800	.3192
CD	1.39*E*-05	1	1.39*E*-05	0.0010	.9754
CE	0.0027	1	0.0027	0.1947	.6669
DE	0.1119	1	0.1119	8.0072	.0152
ABC	1.0221	1	1.0221	73.1096	< .0001
BCD	0.0363	1	0.0363	2.5999	.1328
BCE	0.0481	1	0.0481	3.4374	.0885
BDE	0.0217	1	0.0217	1.5521	.2366
CDE	0.0390	1	0.0390	2.7864	.1209
BCDE	0.1421	1	0.1421	10.1667	.0078
Residual	0.1678	12	0.0140		
Total	17.6059	31			

Another factor which supports the utilization of *MMSE* controller is robustness. As shown in Figure 10, when the *PI* controller is utilized, the *ARL* is sensitive to changes in θ. As a result, the *ARL* significantly increases as the value of θ changes from -0.9 to 0.9. Moreover, at the low θ level (-0.9), the *ARL* is considerably lower than the one at the high θ level (0.9). However, there is no significant difference

Table 4: *ANOVA* for *ARL*.

Source	Sum of Squares	Df	Mean Square	*F* Value	*P*-value
A-θ	626.4130	1	626.4130	10.3963	.0039
B-Shift	1897.2070	1	1897.2070	31.4870	< .0001
C-Controller	153.2251	1	153.2251	2.5430	.1251
E-Signal	4315.0590	1	4315.0590	71.6149	< .0001
AC	968.6924	1	968.6924	16.0769	.0006
BC	70.7281	1	70.7281	1.1738	.2903
BE	709.4874	1	709.4874	11.7750	.0024
CE	7.4518	1	7.4518	0.1237	.7284
BCE	642.6495	1	642.6495	10.6657	.0035
Residual	1325.5800	22	60.2536		
Total	10716.4900	31			

in the value of *ARL* when *MMSE* controller is integrated with the *SPC* system since the *MMSE* controller is not just only robust to the autocorrelation change but also outperforms the *PI* controller in term of *ARL* minimization. In addition, both controllers cause no difference in the *ARL* when θ is low. However, when θ is high, the *MMSE* controller causes a lower *ARL* than the one when the *PI* controller is utilized.

5. Summary and Conclusions

This paper focuses on the in-depth analysis of an integrated control system in order to quantify the effects of the selected factors on autocorrelated process. According to the analysis, the disturbance model, *ARIMA (0, 1, 1)*, effects on the responses have been quantified. In addition, appropriate types of controllers, types of control charts, and types of monitored signals have been determined. In summary, the above analysis is concluded as follows.

(1) For *ARL* response, the *MMSE* controller should be utilized since it is robust to the change in θ, that is, the *ARL*s are not significantly different at the low and high level θ. Moreover, at the different levels of shift sizes and θ, the *MMSE* controller has an equivalent or better potential to minimize *ARL* than the *PI* controller.

(2) The performance of the integrated system to minimize *ARL* will be significantly improved if an *SPC* chart is utilized to monitor control signal rather than error signal.

(3) The types of control charts, *MR* or *EWMA*, utilized in the integrated system have no significant effect on *ARL*.

(4) The minimization of *MSE* is not only affected by the shift magnitude but also by the level of correlation (θ).

(5) The most appropriate combination of the integrated system to minimize *MSE* is the utilization of Shewhart *MR* chart with an *MMSE* controller.

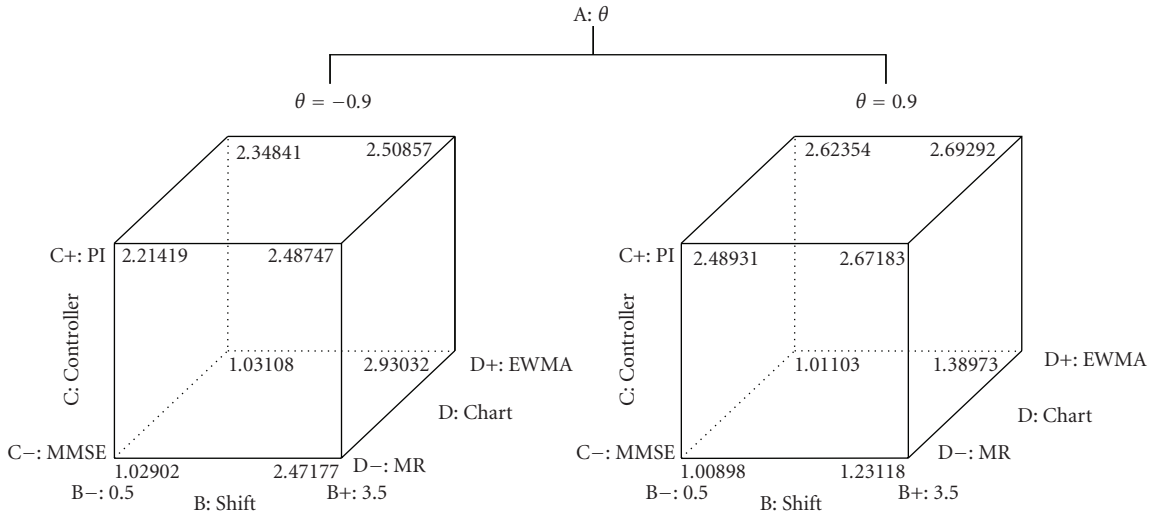

Figure 7: Cube plots of the *BCD* interaction at different θ (for *MSE* response).

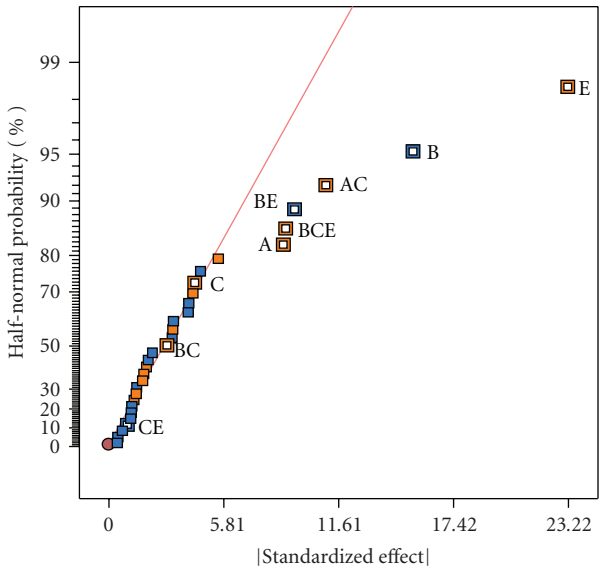

Figure 8: Half-normal plot of effects (for *ARL* response).

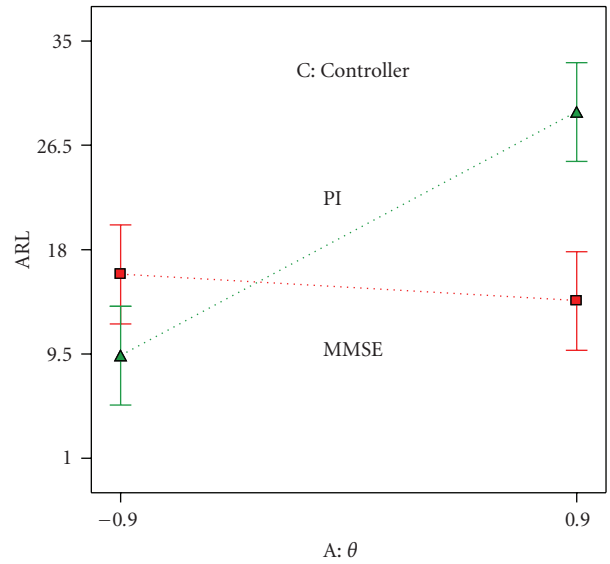

Figure 10: Interaction plot of θ and control charts (for *ARL* response).

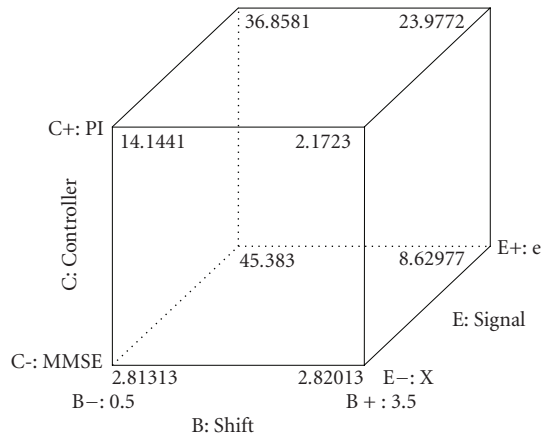

Figure 9: Cube plot of the *BCE* interaction (for *ARL* response).

The analysis performed in this research has suggested essential guidelines to implement the integrated *SPC* effectively. An extension of the research might include the utilization of different process models, for example, *ARIMA (1, 0, 0)*, which represent stationary disturbances.

6. Discussion

Because of the limitation of *SPC*, *APC* methodology, which focuses on the adjustment of the process with the frequency that ensures the lowest deviation from the target, is integrated with *SPC* to solve the correlation and assignable cause problems. According to *APC*, the correlation embedded in the observations will be predicted by fitting the appropriate forecasting model to the correlated data. The integrated

moving average (*IMA*) is a class of forecasting models for monitoring correlated observations and it is proved to best represent process disturbances because of its flexibility. In this study, a simulation model was developed to represent system performance in terms of the mean squared error (*MSE*) of the resulting output and the average run length (*ARL*) of the *SPC* chart utilized. Simulated results were analyzed to identify influential factors likely to affect the system performance. In practical, if the process considered was correctly characterized by the integrated moving average (*IMA*) model. The integrated *SPC* and *APC* is a powerful technique to maintain the process mean on the target. However, the continuous improvement of the model is required in order to ensure the accuracy of the *IMA* model, since the process model has no specific pattern over periods of time.

References

[1] J. F. MacGregor, "On-line statistical process control," *Chemical Engineering Progress*, vol. 84, no. 10, pp. 21–31, 1988.

[2] G. E. P. Box and G. M. Jenkins, *Time Series Analysis: Forecasting and Control*, Holden-day, San Francisco, Calif, USA, 1970.

[3] D. C. Montgomery, J. B. Keats, G. C. Runger, and W. S. Messina, "Integrating statistical process control and engineering process control," *Journal of Quality Technology*, vol. 26, no. 2, pp. 79–87, 1994.

[4] G. E. P. Box and A. Luceno, *Statistical Control by Monitoring and Feedback Adjustment*, John Wiley & Sons, New York, NY, USA, 1997.

[5] C.-W. Lu and M. R. Reynolds Jr., "EWMA control charts for monitoring the mean of autocorrelated processes," *Journal of Quality Technology*, vol. 31, no. 2, pp. 166–188, 1999.

[6] J. R. English, S.-C. Lee, T. W. Martin, and C. Tilmon, "Detecting changes in autoregressive processes with $\overline{X}$ and EWMA charts," *IIE Transactions*, vol. 32, no. 12, pp. 1103–1113, 2000.

[7] D. C. Montgomery, *Introduction to Statistical Quality Control*, John Wiley & Sons, New York, NY, USA, 1997.

[8] G. Taguchi, E. A. ElSayed, and T. C. Hsiang, *Quality Engineering in Production Systems*, McGraw–Hill, New York, NY, USA, 1989.

[9] W. Jiang and K.-L. Tsui, "SPC monitoring of MMSE- and PI-controlled processes," *Journal of Quality Technology*, vol. 34, no. 4, pp. 384–398, 2002.

[10] H. B. Nembhard, "Simulsion using the state-space representation of noisy systems to determine effective integrated process control designs," *IIE Transactions*, vol. 30, no. 3, pp. 247–256, 1998.

[11] C. Capilla, A. Ferrer, R. Romero, and A. Hualda, "Integration of statistical and engineering process control in a continuous polymerization process," *Technometrics*, vol. 41, no. 1, pp. 14–28, 1999.

[12] M. Gultekin, E. A. Elsayed, J. R. English, and A. S. Hauksottir, "Monitoring automatically controlled processes using statistical control charts," *International Journal of Production Research*, vol. 40, no. 10, pp. 2303–2320, 2002.

[13] G. Runger, M. C. Testik, and F. Tsung, "Relationships among control charts used with feedback control," *Quality and Reliability Engineering International*, vol. 22, no. 8, pp. 877–887, 2006.

[14] K. Kandananond, *Performance characterization of integrated statistical process control systems*, Ph.D. dissertation, Wichita State University, 2007.

[15] K. Kandananond, "The effect of autocorrelation (Stationary Data) on the integrated statistical process control system," in *Proceedings of the 3rd World Conference on Production and Operations Management*, pp. 2433–2439, Tokyo, Japan, 2008.

[16] J. F. MacGregor, "A different view of the funnel experiment," *Journal of Quality Technology*, vol. 22, no. 4, pp. 255–259, 1990.

[17] T. J. Harris and W. H. Ross, "Statistical process control procedures for correlated observations," *Canadian Journal of Chemical Engineering*, vol. 69, no. 1, pp. 48–57, 1991.

[18] M. Janakiram and J. B. Keats, "Combining SPC and EPC in a hybrid industry," *Journal of Quality Technology*, vol. 30, no. 3, pp. 189–200, 1998.

[19] S. O. Duffuaa, S. N. Khursheed, and S. M. Noman, "Integrating statistical process control, engineering process control and Taguchi's quality engineering," *International Journal of Production Research*, vol. 42, no. 19, pp. 4109–4118, 2004.

[20] S. Bisgaard and M. Kulahci, "Quality quandaries: the effect of autocorrelation on statistical process control procedures," *Quality Engineering*, vol. 17, no. 3, pp. 481–489, 2005.

[21] K. Triantafyllopoulos, J. D. Godolphin, and E. J. Godolphin, "Process improvement in the microelectronic industry by state space modelling," *Quality and Reliability Engineering International*, vol. 21, no. 5, pp. 465–475, 2005.

[22] J. M. Lucas and M. S. Saccucci, "Exponentially weighted moving average control schemes. Properties and enhancements," *Technometrics*, vol. 32, no. 1, pp. 1–12, 1990.